J. Opt. 29 (1998) 324–338. Printed in the UK PII: S0150-536X(98)95748-3

Colour representation spaces at different physiological levels: a comparative analysis

P Capilla†, J Malo, M J Luque and J M Artigas

Dpto Òptica, Facultat de Físiques, Universitat de València, Dr Moliner, 50 46100 Burjassot, València, Spain

Received 11 May 1998, accepted 6 July 1998

Abstract. In this work, we analyse and compare several linear and nonlinear colour representation spaces at different physiological levels, show the relationships between spaces and discuss the mathematical properties they should exhibit. At the photoreceptor level, we examine the *cone excitation* and the *cone contrast spaces*. We discuss the second-stage spaces, usually known as *ATD-spaces*, paying particular attention to Boynton's space and including a nonlinear space, the *opponent modulation space*. In addition, we approach third-stage transformations, which might take place at the cortical level. Finally, we analyse a perceptual *ATD*-type space, discussing how it might be derived as a third-stage transformation of an LGN-based *ATD*-space.

Keywords: Cone excitation spaces, cone contrast space, *ATD*-spaces, opponent modulation space, third-stage spaces

Espaces de représentation de la couleur dans différents niveaux physiologiques: une analyse comparative

Résumé. Dans ce travail, nous analysons et comparons divers espaces linéaires et non linéaires de représentation de la couleur relativement à différents niveaux physiologiques, en montrant des relations entre espaces et en discutant quelles propriétés mathémathiques doivent posséder. Au niveau des photorécepteurs nous examinons *l'espace d'excitation des cônes* et *l'espace de contraste des cônes*. Parmi les espaces à deux niveaux, connus habituellement sous le nom *d'espaces ATD*, nous étudions notamment l'espace de Boynton et un espace nonlinear, *l'espace des modulations opposantes*. Nous considérons aussi les transformations de troisième niveau qui ont lieu au niveau cortical. Finallement, nous analysons un espace perceptif du type *ATD*, en discutant comment un tel espace pourrait être obtenu comme une transformée de troisième niveau d'un espace *ATD* basé sur le NGL.

Mots clés: Espaces d'excitation de cônes, espace de contraste des cônes, espaces *ATD*, espace de modulations opposantes, espaces de troisième niveau

1. Introduction

The aim of colorimetry is to obtain a numerical characterization of colour which is easily computable from the physical characteristics of chromatic stimuli. Such characterization must verify two basic properties to be useful. First, it must be a one-to-one mapping, that is, each colour C must be unequivocally characterized by a set of numerical values $T(C) = (T_1(C), T_2(C), \ldots, T_n(C))$. Second, the characterization must be *powerful*, that is, it must be possible to infer physical properties from the numerical representation. For example, the definition of 'distance' from the numerical representation, $d(T(C_1), T(C_2))$, should have perceptual meaning. We are aiming, then, to represent colour in a *metric space* (Edwards 1973). Also, it is desirable that changes in the stimulus can be described by mathematical operations in

† E-mail address: Pascual.Capilla@uv.es

0150-536X/98/050324+15$19.50 © 1998 IOP Publishing Ltd

the representation space. Thus, for instance, a luminance increase in colour C_1 by a factor k (let us say $C_2 = kC_1$), a colour mixture ($C_3 = C_4 + C_5$) or a spatial configuration change of the chromatic stimulus ($C_7 = S(C_6)$), must have their numerical equivalent in the representation space, in such a way that $T(C_2) = kT(C_1)$, $T(C_3) = T(C_4) + T(C_5)$ and $T(C_7) = S(T(C_6))$.

The properties verified by these operations determine the *mathematical structure* of the space (Edwards 1973). The greater the complexity of the space structure, the wider the range of phenomena that can be represented by that space. The usefulness of a given representation is related to the degree up to which colour verifies the mathematical properties defining such a representation. For instance, if we want to represent *colour phenomena* in a *vector space*, the linearity axiom required by the vector character may limit the applicability of the representation to restricted experimental conditions. Therefore, the principle underlying the choice of a particular numerical colour representation is a compromise between mathematical power (that is, the capability to make quantitative predictions) and generality.

The more widely used colour representation is based on the properties of trichromatic matching in isolated fields of controlled geometry (Grassmann's laws (Wyszecki and Stiles 1982, pp 117–248)). These properties favour a three-dimensional colour representation, with *tristimulus vectors*. The metric of this space is clearly non-Euclidean, as can be seen when discrimination thresholds are represented in the tristimulus space (Brown and MacAdam 1949). A three-dimensional vector representation with a Riemmanian metric (Dubrovin *et al* 1984) is mathematically more powerful, but it still does not include fundamental phenomena such as the nonlinearity of the visual system (adaptation for instance), chromatic induction and colour constancy. To take into account these phenomena, additional parameters, such as information about the illuminant or the stimulus' spatial configuration, ought to be included. Consequently, the complexity of the mathematical structure of the representation would increase considerably.

All the representations obtained from linear transformations of the tristimulus vectors may be interpreted as a basis transformation. Though any set of primaries is valid to compute additive mixtures, the usefulness of each representation will depend, among other things, on the meaning of the basis vectors, the metric characteristics of the resulting space or the statistical properties of the visual stimuli to be analysed. Different linear representations are more useful for different applications.

Not all three-dimensional representations are vector spaces—the characterizations by chromaticity coordinates and luminance or dominant wavelength, colorimetric purity and luminance, for instance—nor is it always advantageous to keep the vector character. For example, if the tristimulus space is not Euclidean, we will not be able to obtain a uniform representation by linear transformations (Dubrovin *et al* 1984). Thus, the uniform spaces recommended by the CIE ($L^*u^*v^*$ and $L^*a^*b^*$—1976) (Wyszecki and Stiles 1982, pp 486–513), or the more recent *Rlab* (Fairchild and Berns 1993, Fairchild 1996), *Llab* (Luo *et al* 1996) or SVF (Seim and Valberg 1986) for instance, involve nonlinear transformations, and are not, therefore, vector spaces. On the other hand, a linear increment of the stimulus causes a nonlinear detector response increment in the visual system, so any colour representation aiming to reproduce physiological responses to incremental stimuli on a given pedestal must necessarily be nonlinear.

In the present work, we analyse from a unified point of view some of the main linear colour representations at different physiological levels: photoreceptors (*excitation spaces*), opponent and non-opponent cells at the lateral geniculate nucleus (LGN) (*ATD-spaces*) and primary cortex. Two different ways of dealing with the nonlinearities of the visual system have, nevertheless, been included: a nonlinear representation with a matrix dependent on the adapting background stimulus (*opponent modulation space*), and a more complex model that explicitly proposes adaptation and signal compression mechanisms (Guth 1991). In particular, we discuss both the usefulness of the background-dependent transform as a colour representation and the mathematical properties it should verify. The global view given of the different colour representation spaces may be useful not only for colour vision research, but also for an interdisciplinary scientific community increasingly interested in colour problems. The advantages arising from taking into account the properties of the visual system in image processing were demonstrated quite early on (Stockham 1972, Faugeras 1979). In this context, visual system models have an increasingly wide range of recent applications (Bumbaca and Smith 1987, Sharma and Trusell 1997, Ebrahimi and Kunt 1998), including, for instance, efficient encoding of colour images in limited-bandwidth channels (Blinn 1993, Léger *et al* 1991), optimum colour space quantization for palette design (Balasubramanian *et al* 1994, Wan *et al* 1990) and pattern recognition (Lee *et al* 1994, Liu *et al* 1996, Millan *et al* 1995).

2. Cone-based spaces

2.1. Cone excitation spaces

It can be proved (Estévez 1979) that the cone space primaries (L, M, S), are the confusion points of the three kinds of dichromats—protanopes, deuteranopes and tritanopes—assuming that dichromacy arises from lack of one of the three cone types (long, medium or short for protanopes, deuteranopes and tritanopes, respectively). This is known as *König's hypothesis* (Wyszecki and Stiles 1982, pp 582–689). Therefore, the equation that defines the basis transformation from the XYZ tristimulus values to the LMS cone responses is

$$\begin{pmatrix} X \\ Y \\ Z \end{pmatrix} = \begin{pmatrix} X_{cp} & X_{cd} & X_{ct} \\ Y_{cp} & Y_{cd} & Y_{ct} \\ Z_{cp} & Z_{cd} & Z_{ct} \end{pmatrix} \begin{pmatrix} L \\ M \\ S \end{pmatrix} \qquad (1)$$

Table 1.

	x_{cp}	y_{cp}	x_{cd}	y_{cd}	x_{ct}	y_{ct}
Vos and Walraven	0.7465	0.2535	1.4000	−0.4000	0.1747	0.0060
Smith and Pokorny	0.7465	0.2535	1.4000	−0.4000	0.1748	0.0000

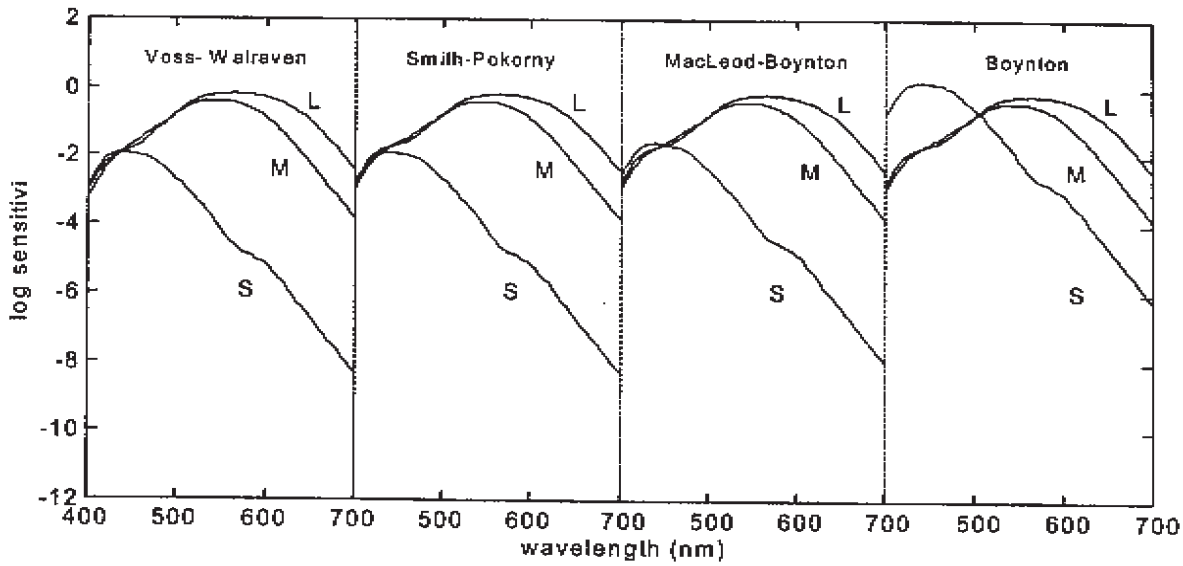

Figure 1. König-type fundamentals computed with different constraints on the *S*-cones: (*a*) Vos and Walraven; (*b*) Wyszecki and Stiles; (*c*) MacLeod and Boynton; (*d*) Boynton.

where (X_{cp}, Y_{cp}, Z_{cp}), (X_{cd}, Y_{cd}, Z_{cd}) and (X_{ct}, Y_{ct}, Z_{ct}) are the components of the confusion points of protanopes, deuteranopes and tritanopes, respectively. If the chromaticity coordinates of these points are known (see table 1) and since coordinates and components are proportional, equation (1) can be written as

$$\begin{pmatrix} X \\ Y \\ Z \end{pmatrix} = \begin{pmatrix} x_{cp} & x_{cd} & x_{ct} \\ y_{cp} & y_{cd} & y_{ct} \\ z_{cp} & z_{cd} & z_{ct} \end{pmatrix} \begin{pmatrix} k_{cp} & 0 & 0 \\ 0 & k_{cd} & 0 \\ 0 & 0 & k_{ct} \end{pmatrix} \begin{pmatrix} L \\ M \\ S \end{pmatrix} \tag{2}$$

where k_{cp}, k_{cd} and k_{ct} are arbitrary scaling constants. If we solve (2) for LMS, we obtain

$$\begin{pmatrix} L \\ M \\ S \end{pmatrix} = \begin{pmatrix} k'_{cp} & 0 & 0 \\ 0 & k'_{cd} & 0 \\ 0 & 0 & k'_{ct} \end{pmatrix} \begin{pmatrix} x_{cp} & x_{cd} & x_{ct} \\ y_{cp} & y_{cd} & y_{ct} \\ z_{cp} & z_{cd} & z_{ct} \end{pmatrix}^{-1} \begin{pmatrix} X \\ Y \\ Z \end{pmatrix} \tag{3}$$

where $k'_{cp} = 1/k_{cp}$, $k'_{cd} = 1/k_{cd}$ and $k'_{ct} = 1/k_{ct}$.

Once the coordinates of the confusion points and the scaling constraints have been chosen, the tristimulus values in the *LMS-space* are defined. If we write equation (3) for the particular case of an equal-energy spectrum, then the tristimulus values (XYZ) will be the colour-matching functions $(\bar{x}_\lambda, \bar{y}_\lambda, \bar{z}_\lambda)$ and the corresponding LMS values will be the spectral sensitivities, $S_L(\lambda)$, $S_M(\lambda)$, $S_S(\lambda)$, of the L, M and S mechanisms, respectively. These are usually called *König fundamentals* (Wyszecki and Stiles 1982, pp 582–689):

$$\begin{pmatrix} S_L(\lambda) \\ S_M(\lambda) \\ S_S(\lambda) \end{pmatrix} = \begin{pmatrix} k'_{cp} & 0 & 0 \\ 0 & k'_{cd} & 0 \\ 0 & 0 & k'_{ct} \end{pmatrix} \times \begin{pmatrix} x_{cp} & x_{cd} & x_{ct} \\ y_{cp} & y_{cd} & y_{ct} \\ z_{cp} & z_{cd} & z_{ct} \end{pmatrix}^{-1} \begin{pmatrix} \bar{x}_\lambda \\ \bar{y}_\lambda \\ \bar{z}_\lambda \end{pmatrix}. \tag{4}$$

Although numerous derivations of such fundamentals can be found in the literature (Estévez 1979, Wyszecki and Stiles 1982, pp 582–689, Stockman *et al* 1993, Vos and Walraven 1971, Walraven 1974, Vos 1978, Smith and Pokorny 1975, DeMarco *et al* 1992), we will discuss only those by Vos and Walraven (Vos and Walraven 1971, Walraven 1974, Vos 1978) and by Smith and Pokorny (Smith and Pokorny 1975, DeMarco *et al* 1992), which are the most widely used. Vos and Walraven's fundamentals (figure 1) are computed with the condition that luminance, Y, equals $L + M + S$. In other words, the spectral sensitivities of the fundamentals sum to the spectral sensitivity curve, V_λ. With this condition, equation (3) becomes

$$\begin{pmatrix} L \\ M \\ S \end{pmatrix} = \begin{pmatrix} 0.15516 & 0.54308 & -0.03702 \\ -0.15516 & 0.45692 & 0.02969 \\ 0 & 0 & 0.00732 \end{pmatrix} \begin{pmatrix} X' \\ Y' \\ Z' \end{pmatrix} \tag{5}$$

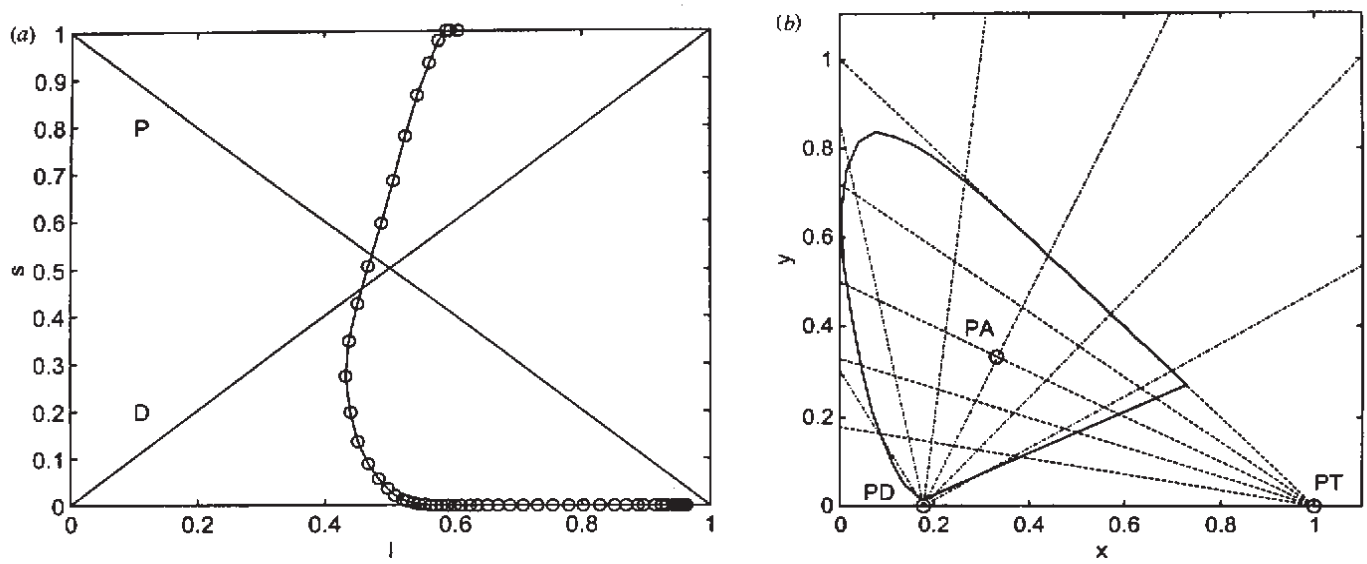

Figure 2. (*a*) MacLeod–Boynton diagram, showing the spectral locus. The lines passing through (1, 0) and (0, 0) are, respectively, a protanopic (*P*) and a deuteranopic (*D*) confusion line. (*b*) Constant *L* and *M* lines converging at the tritanopic confusion point, and constant *S* lines converging at point (1, 0). The points labelled (*PA*), (*PT*) and (*PD*) define the basis of primaries in Boynton's space.

where (X', Y', Z') are the XYZ tristimulus values including Judd's modification (Judd 1951).

Smith and Pokorny required that $Y = L + M$, that is, $V_\lambda = S_L(\lambda) + S_M(\lambda)$, but the scaling condition for the *S*-cones was open. The constraint on luminance is consistent with physiological evidence suggesting that *S*-cones do not contribute to luminance (Eisner and MacLeod 1980, Tansley and Boynton 1976, 1978), although results to the contrary can also be found in the literature (Drum 1983). This scaling condition on luminance automatically implies that

$$S_L(570) - 2S_M(570) = 0. \tag{6}$$

From equation (3), Smith and Pokorny's fundamentals have the following general form (Smith and Pokorny 1996):

$$\begin{pmatrix} L \\ M \\ S \end{pmatrix} = \begin{pmatrix} 0.15514 & 0.54312 & -0.03286 \\ -0.15514 & 0.45684 & 0.03286 \\ 0 & 0 & a_{33} \end{pmatrix} \begin{pmatrix} X' \\ Y' \\ Z' \end{pmatrix}. \tag{7}$$

The scaling condition for *S*-cones obeys different criteria. For instance Wyszecki and Stiles, following Vos and Walraven (1971), use the condition (Wyszecki and Stiles 1982, pp 582–689):

$$S_L(475.5) + S_M(475.5) = 16S_S(475.5). \tag{8}$$

Conditions (6) and (8) are not arbitrary. They are based on the invariant hues, blue and yellow, observed at 475.5 and 570 nm, respectively, observed by Walraven (1961). From (8) and (7)

$$\begin{pmatrix} L \\ M \\ S \end{pmatrix} = \begin{pmatrix} 0.15514 & 0.54312 & -0.03286 \\ -0.15514 & 0.45684 & 0.03286 \\ 0 & 0 & 0.00801 \end{pmatrix} \begin{pmatrix} X' \\ Y' \\ Z' \end{pmatrix}. \tag{9}$$

Wyszecki–Stiles' fundamentals are shown in figure 1.

Another possibility is to assume that

$$S_L(400) + S_M(400) = S_S(400). \tag{10}$$

This condition, which we will discuss below, yields

$$\begin{pmatrix} L \\ M \\ S \end{pmatrix} = \begin{pmatrix} 0.15514 & 0.54312 & -0.03286 \\ -0.15514 & 0.45684 & 0.03286 \\ 0 & 0 & 0.01608 \end{pmatrix} \begin{pmatrix} X' \\ Y' \\ Z' \end{pmatrix} \tag{11a}$$

$$\begin{pmatrix} L \\ M \\ S \end{pmatrix} = \begin{pmatrix} 0.15516 & 0.54308 & -0.03287 \\ -0.15516 & 0.45692 & 0.03287 \\ 0 & 0 & 0.01608 \end{pmatrix} \begin{pmatrix} X' \\ Y' \\ Z' \end{pmatrix} \tag{11b}$$

where X', Y' and Z' are, in equation (11*a*), the XYZ tristimulus values as modified by Judd (1951) and in equation (11*b*) those refined by Vos (1978), which will be used in what follows. These fundamentals (figure 1) define the well known *MacLeod–Boynton* space (MacLeod and Boynton 1979), also known as *cone excitation space*. From the LMS tristimulus values, the (l, m, s) coordinates in the excitation space are defined as follows:

$$l = \frac{L}{L+M} \qquad m = \frac{M}{L+M} \qquad s = \frac{S}{L+M}. \tag{12}$$

With the normalization condition (10), the s coordinate is between 0 and 1. In figure 2(*a*), we plot the spectral locus in an (l, s)-plane of constant luminance. This is not strictly a chromatic diagram, since it is not contained on a constant $L + M + S$ plane, but in a constant $L + M$ plane. Nevertheless, it is usually called the *MacLeod–Boynton diagram*. In this diagram, the lines converging at the points (0, 0) and (1, 0) are deuteranopic and protanopic confusion lines, respectively, since in the cone excitation space these points are the confusion centres (0, 1, 0) and (1, 0, 0).

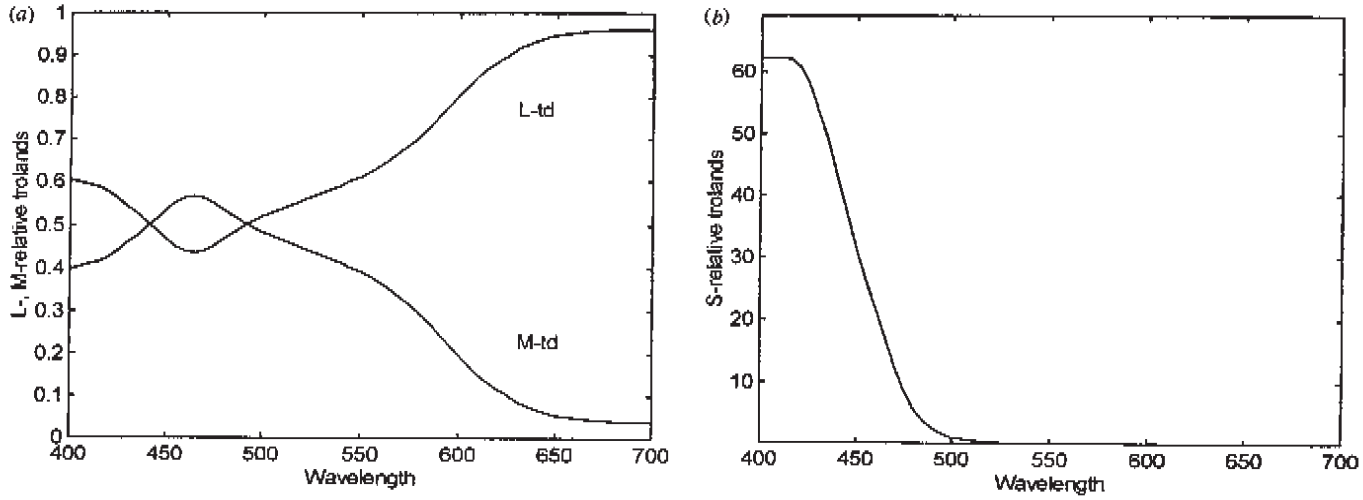

Figure 3. Cone-trolands coordinates (Boynton–Kambe) as a function of wavelength. (*a*) *L*- and *M*-trolands. (*b*) *S*-trolands.

It is useful to interpret the meaning of certain loci in this diagram. For instance, L and M are constant along any vertical line, and obviously the ratio between L and M or any linear combination of L and M is also constant. Therefore, if only S changes along a vertical line, a subject deprived of the short-wavelength cones would be unable to discriminate between any two colours on that line, which is therefore a tritanopic confusion line. On the other hand, S is constant in any horizontal line and therefore any linear combination $k_1(L + M) + k_2S$ is also constant—let us remember that we are in a constant $L + M$ plane. After a little algebra, it can be shown that these lines on the (l, s) diagram correspond to the lines in the (x, y) diagram defined by the following equations:

$$S = \text{constant} \quad \Rightarrow \quad y = \frac{(1-x)}{1 + [1.021\,3048/(L+M)]S} \tag{13}$$

$$L, M = \text{constant} \quad \Rightarrow \quad y = \frac{1.24(1 + L/M)(x - 0.175)}{2.79L/M - 3.79}. \tag{14}$$

Therefore, vertical lines on the (l, s)-diagram are transformed in the (x, y)-diagram into lines converging at the point of coordinates $(0.175, 0)$ (see figure 2(*b*)), which will then be the tritanopic confusion point. In particular, the tritanopic confusion line going through the white point, $(\frac{1}{3}, \frac{1}{3})$, intersects the spectral locus at 570 nm. On the other hand, the horizontal lines are transformed into lines converging to the point of coordinates $(1, 0)$, and, in particular, the line of constant S passing through white intersects the locus at 498 nm. It is possible to take advantage of this result to propose, as in Boynton's model (Boynton 1986), the following alternative to equation (10):

$$S_L(498) + S_M(498) = S_S(498). \tag{15}$$

The justification of this condition will become clear when discussing the *ATD*-spaces.

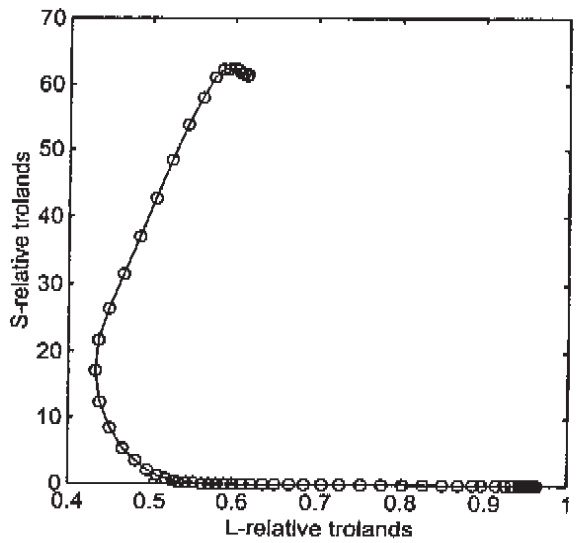

Figure 4. Boynton–Kambe diagram, showing the spectral locus.

From equation (15), $a_{33} = 1$, and thus equation (7) becomes

$$\begin{pmatrix} L \\ M \\ S \end{pmatrix} = \begin{pmatrix} 0.155\,16 & 0.543\,08 & -0.032\,87 \\ -0.155\,16 & 0.456\,92 & 0.032\,87 \\ 0 & 0 & 1.006\,6 \end{pmatrix} \begin{pmatrix} X \\ Y \\ Z \end{pmatrix}. \tag{16}$$

Equation (16) defines the Boynton space fundamentals. The spectral sensitivities of these fundamentals are shown in figure 1.

A characterization alternative to the chromatic coordinates l, m, s are the L-, M- and S-trolands. Let us consider a stimulus, producing a retinal illumination level E, in trolands. The magnitudes L- and M-trolands (L-td and M-td) are defined as the product of E and the l and m coordinates. Naturally, L-td and M-td sum to the retinal illumination. The magnitude S-troland (S-td) requires a different treatment, since the S-cones do not contribute to luminance. Boynton and Kambe (1980) define 1 S-td as the excitation produced in the S-cones by an achromatic

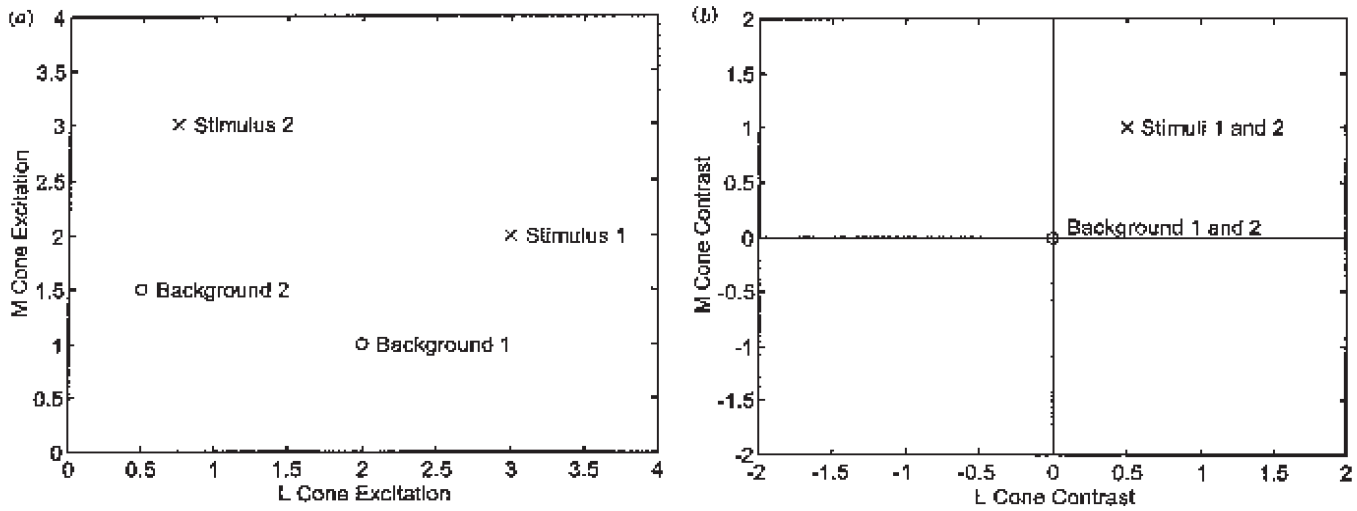

Figure 5. Two incremental stimuli with different backgrounds plotted in (*a*) the cone excitation space and (*b*) the cone contrast space. Note that both signals plot in the same point of the cone contrast space, since the information about the background is lost.

stimulus (the equal-energy white) of 1 td. With all this, we may finally write

$$\begin{aligned} L\text{-td} &= El \\ M\text{-td} &= Em \\ S\text{-td} &= Es. \end{aligned} \tag{17}$$

The L-, M- and S-td coordinates define the *cone-trolands* space or *Boynton–Kambe* space. Figure 3(*a*) shows L-td and M-td per troland as a function of wavelength. Note that both curves are mirror images. The variation of the magnitude S-td with wavelength appears in figure 3(*b*). With Boynton's fundamentals, we may also derive a Boynton–Kambe diagram. Note that in this case, the S-td coordinate (figure 4) is not between 0 and 1, as in the MacLeod–Boynton diagram, but between 0 and 62, approximately.

2.2. Cone contrast space

Let us consider a visual stimulus defined by its (L_0, M_0, S_0) components in the cone excitation space. We aim to characterize an incremental signal $(\Delta L, \Delta M, \Delta S)$ on that stimulus, which we will call 'background'. We may represent both background and signal in the cone excitation space (figure 5(*a*)), but, alternatively, the signal may be represented in a new space, the *cone contrast space* (Stromeyer *et al* 1983, 1985), defined by the quantities $(\Delta L/L_0, \Delta M/M_0, \Delta S/S_0)$. In this space, the background is the origin of coordinates, and therefore the information about (L_0, M_0, S_0) is lost (figure 5(*b*)). Note that this representation space, unlike the cone excitation space, is not a vector space.

3. Second-stage spaces

3.1. *ATD*-spaces

The photoreceptor signals are recombined from the ganglion cells and transmitted to the LGN without relevant distortion. So, from a functional point of view, both levels may be considered as equivalent. The result of such recombinations is a new set of three signals—one achromatic and two chromatic ones, whose physiological support would be the non-opponent and opponent cells, respectively (Wiesel and Hubel 1966, DeValois *et al* 1966, Gouras 1968, DeMonasterio and Gouras 1975, Creutzfeldt *et al* 1979, Lee *et al* 1987).

Some colour vision models aim to reproduce the performance of the opponent and non-opponent cells with linear combinations of the LMS cone responses. These are the LGN-based models (Ingling and Tsou 1977, Boynton 1986). Nevertheless, other models (Jameson and Hurvich 1955a, Hurvich and Jameson 1957, Guth *et al* 1980), define cone transformations that, under certain constraints, adequately predict discrimination thresholds and colour appearance properties. Although there is not an explicit relationship between such transformations and the responses of a given class of cells, the notation employed is usually that of the LGN-based models. Following Guth and co-workers (Guth *et al* 1980), usually A is the achromatic signal, T the red–green opponent signal and D the yellow–blue opponent signal.

The transformation from LMS to ATD presents the following general form:

$$\begin{pmatrix} A \\ T \\ D \end{pmatrix} = \begin{pmatrix} a_{11} & a_{12} & a_{13} \\ a_{21} & a_{22} & a_{23} \\ a_{31} & a_{32} & a_{33} \end{pmatrix} \begin{pmatrix} L \\ M \\ S \end{pmatrix}. \tag{18}$$

The particular form of equation (18) changes with the model. Thus, for instance, in the model of Jameson and Hurvich (1955a) and Hurvich and Jameson (1957), equation (18) is written as

$$\begin{pmatrix} A \\ T \\ D \end{pmatrix} = \begin{pmatrix} k_1 & 0 & 0 \\ 0 & k_2 & 0 \\ 0 & 0 & k_3 \end{pmatrix} \begin{pmatrix} 1 & 1 & 1 \\ 1 & -2 & 1 \\ -2 & 1 & 1 \end{pmatrix} \begin{pmatrix} L \\ M \\ S \end{pmatrix} \tag{19}$$

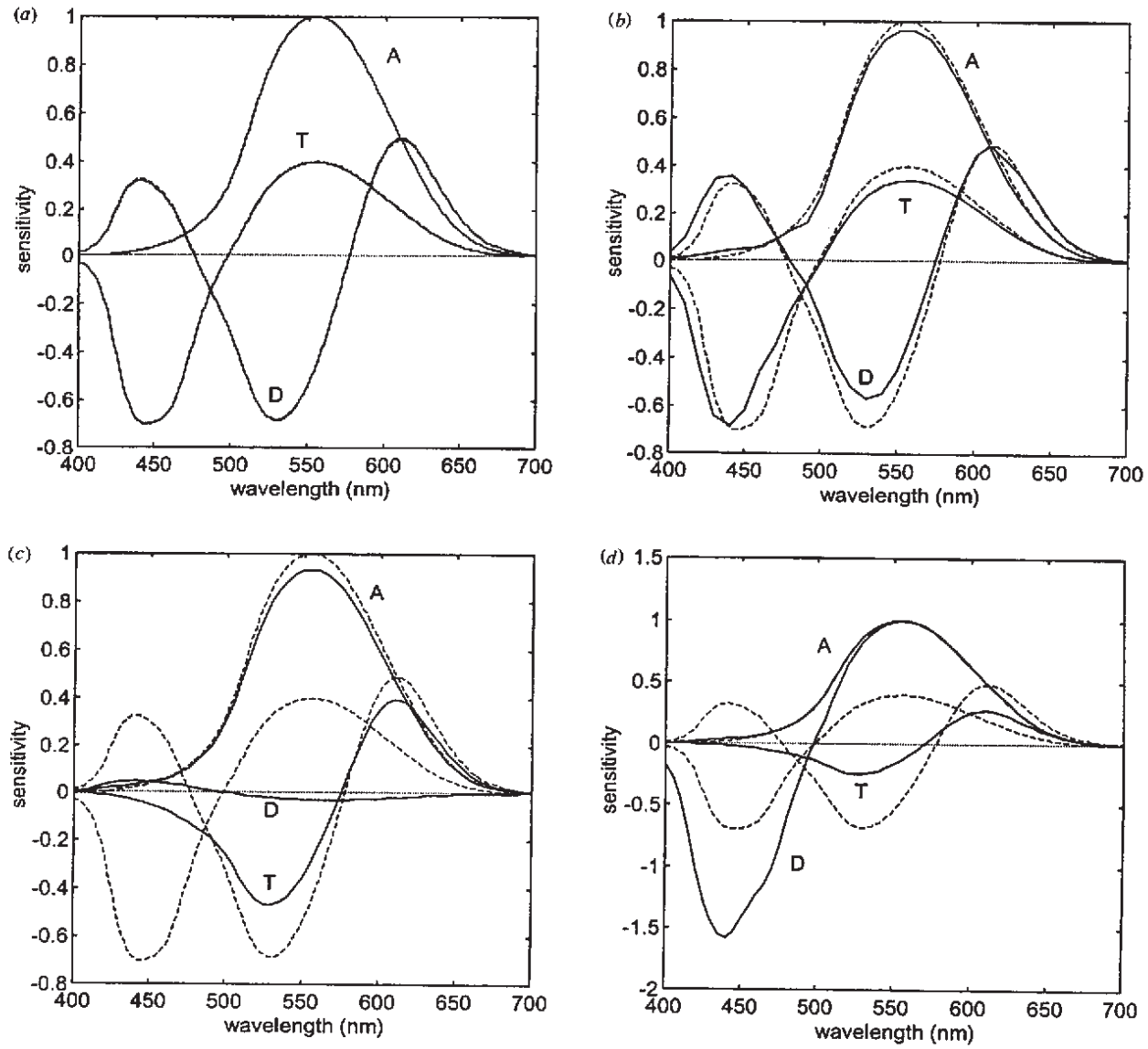

Figure 6. Spectral sensitivities of the *A*, *T* and *D* channels (full curves) compared with the curves from Jameson and Hurvich's hue cancellation experiment (Jameson and Hurvich 1955a, b) and the spectral luminous efficiency function (broken curves). (*a*) Jameson and Hurvich (1955a, b), (*b*) Ingling and Tsou (1977), (*c*) Guth *et al* (1980), (*d*) Boynton (1986).

where k_1, k_2 and k_3 are adaptation-dependent normalizing constants and LMS is given by

$$\begin{pmatrix} L \\ M \\ S \end{pmatrix} = \begin{pmatrix} 0 & 6.5341 & 0.1336 \\ -0.3368 & 7.0009 & 0.0020 \\ 0.3329 & 6.4671 & -0.1347 \end{pmatrix} \begin{pmatrix} X \\ Y \\ Z \end{pmatrix}. \tag{20}$$

In the original version of their model, Jameson and Hurvich speak of photochemical decomposition of substances at certain post-receptoral sites. However, on the basis of more recent evidence, this transform may be interpreted as neural transformations occurring at an unspecified site. For a revision of this model see Jameson and Hurvich (1968).

In the model proposed by Guth and co-workers (Guth *et al* 1980), which, though considering *ATD* neural transformations, does not specify either of the underlying cells, equation (18) takes the following form:

$$\begin{pmatrix} A \\ T \\ D \end{pmatrix} = \begin{pmatrix} k_1 & 0 & 0 \\ 0 & k_2 & 0 \\ 0 & 0 & k_3 \end{pmatrix} \times \begin{pmatrix} 0.5967 & 0.3654 & 0 \\ 0.9553 & -1.2836 & 0 \\ -0.0284 & 0 & 0.0483 \end{pmatrix} \begin{pmatrix} L \\ M \\ S \end{pmatrix} \tag{21}$$

where k_1, k_2 and k_3 are adaptation-dependent weightings (at absolute threshold conditions, their value is unity) and LMS are the Smith–Pokorny fundamentals, normalized to unity at their peaks:

$$\begin{pmatrix} L \\ M \\ S \end{pmatrix} = \begin{pmatrix} 0.2434 & 0.8524 & -0.0516 \\ -0.3954 & 1.1642 & 0.0837 \\ 0 & 0 & 0.6225 \end{pmatrix} \begin{pmatrix} X' \\ Y' \\ Z' \end{pmatrix}. \tag{22}$$

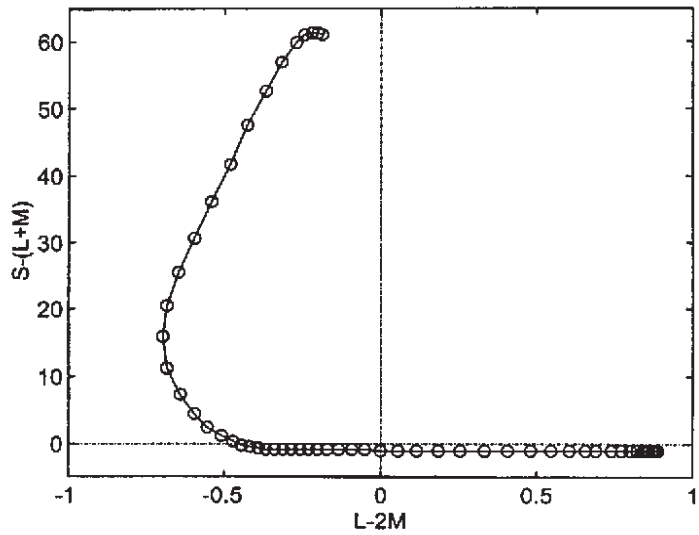

Figure 7. Diagram of $L-2M$ and $S-(L+M)$ coordinates in a constant A plane, showing the spectral locus and the null axes of the T and D channels.

A useful table containing these fundamentals in 1 nm steps can be found in the paper by DeMarco *et al* (1992).

The model proposed by Ingling and Tsou (1977), gives the following form for equation (18):

$$\begin{pmatrix} A \\ T \\ D \end{pmatrix} = \begin{pmatrix} 0.60 & 0.40 & 0 \\ 1.20 & -1.60 & 0.40 \\ 0.24 & 0.105 & -0.70 \end{pmatrix} \begin{pmatrix} L \\ M \\ S \end{pmatrix} \qquad (23a)$$

$$\begin{pmatrix} A \\ T \\ D \end{pmatrix} = \begin{pmatrix} 0.60 & 0.40 & 0 \\ 1.20 & -1.60 & 0 \\ 0.048 & -0.039 & -0.042 \end{pmatrix} \begin{pmatrix} L \\ M \\ S \end{pmatrix}. \qquad (23b)$$

Equation (23*a*) is valid for supra-threshold and white-light-adapted stimuli and (23*b*) for threshold and dark-adapted stimuli (Ingling 1977). LMS are again the Smith–Pokorny fundamentals normalized to unity, but in a slightly modified version differing from (21) in the short-wave limbs of the L- and M-curves. The corresponding values, tabulated in 10 nm steps, can be found in Ingling and Tsou (1977).

The spectral sensitivities of the A, T and D channels are shown in figures 6(*a*)–(*c*). The main differences between these models are the contribution of S to luminance and the T channel and the contribution of M to the D channel. As we discussed when introducing Smith and Pokorny's fundamentals, there is evidence both for and against the contribution of S to channel A, though mostly supporting the idea that S does not contribute to luminance (see above). Regarding the contribution of S to T, whereas Hurvich and Jameson's and Ingling and Tsou's models are in agreement with the data from hue cancellation and hue naming experiments (Jameson and Hurvich 1955b, Ingling *et al* 1978, Wooten and Werner 1978, Boynton *et al* 1964), the model by Guth *et al* is supported by the additivity (Guth *et al* 1969, Kranda and King-Smith 1969) and chromatic selective adaptation (Krauskopf *et al* 1982) experiments. Finally, while from the psychophysical data it can be inferred that M contributes to D (Mollon and Polden 1977, Wisowaty 1983), in disagreement with the hypothesis of Guth and co-workers, from the physiological viewpoint the matter is not completely clear. The inputs for the yellow side for yellow/blue opponency might be just the L-cones (DeValois *et al* 1966), the M-cones (Wiesel and Hubel 1966, Vautin and Dow 1985, Lee *et al* 1987) or the sum of both (DeMonasterio and Gouras 1975, Derrington *et al* 1984). There is even some evidence on the yellow side being provided by the M-cones and the blue side by the S-cones plus a small contribution from the L-cones (Vautin and Dow 1985).

The space more used lately is Boynton's, which is also based on the Smith and Pokorny fundamentals, with the condition that L and M sum up to luminance (Boynton 1986). The achromatic channel is given, therefore, by $L+M$. T and D are required to have neutral points at 570 and 498 nm, respectively, assuming that these wavelengths correspond to the neutral points of the opponent red–green and yellow–blue LGN cells (Wiesel and Hubel 1966, Derrington *et al* 1984). As we have mentioned above, the scaling condition on luminance automatically implies that $L = 2M$ at 570 nm. So, if a neutral point is wanted at that wavelength, the T-channel must be defined as $k_1L + k_2M$ with $k_1 = 1$ and $k_2 = -2$. Finally, the scaling condition on the S-cones (equation (15)) implies that the D-channel will have a neutral point at 498 nm only if it is defined as $k_1(L+M) + k_2S$, with $k_1 = 1$ and $k_2 = -1$. All these considerations determine the new form taken by equation (18):

$$\begin{pmatrix} A \\ T \\ D \end{pmatrix} = \begin{pmatrix} 1 & 1 & 0 \\ 1 & -2 & 0 \\ 1 & 1 & -1 \end{pmatrix} \begin{pmatrix} L \\ M \\ S \end{pmatrix}. \qquad (24)$$

The ATD channels thus defined (see figure 6(*d*)) are consistent with the cardinal directions measured by Krauskopf *et al* (1982) in LGN cells. Note that the main characteristic of this space is that the T channel does not re-emerge in the violet end of the spectrum, in clear disagreement with the spectral sensitivity determined by hue cancellation. This poses a strong problem for some colour appearance predictions. When discussing third-stage spaces, we suggest a possible solution to this problem.

The *ATD* signals may naturally be considered as the tristimulus values in an *ATD-space* whose primaries are, in the XYZ-space, the stimuli isolating the A, T and D channels, namely, the equal-energy spectrum ($x = \frac{1}{3}$, $y = \frac{1}{3}$), which verifies $T = D = 0$, the tritanopic confusion point ($x = 0$, $y = 0.175$), which verifies $A = T = 0$, and the point of coordinates $x = 1$, $y = 0$, which verifies $A = D = 0$ (see figure 2(*b*)). Thus, the matrix of the basis transformation from XYZ to ATD can be written as

$$\begin{pmatrix} A \\ T \\ D \end{pmatrix} = \begin{pmatrix} k_1 & 0 & 0 \\ 0 & k_2 & 0 \\ 0 & 0 & k_3 \end{pmatrix} \begin{pmatrix} \frac{1}{3} & 1 & 0.175 \\ \frac{1}{3} & 0 & 0 \\ \frac{1}{3} & 0 & 0.825 \end{pmatrix}^{-1} \begin{pmatrix} X' \\ Y' \\ Z' \end{pmatrix} \tag{25}$$

where k_1, k_2 and k_3 are scaling constants. In fact, it can be easily proved that equation (25) results from substituting (16) in (24), if only $k_1 = \frac{1}{3}$, $k_2 = 0.4655$ and $k_3 = -0.8304$.

In the cone excitation space, a chromatic diagram was derived at a constant luminance plane. In the same way, in an *ATD*-space a diagram in the same sense, that is, a diagram in a constant A plane, may be proposed. Figure 7 shows the spectral locus in a plane of $T = L - 2M$ and $D = S - (L + M)$ components. As $L + M$ is constant in that plane, we might use as component D the S value only. Nevertheless, other choices are also possible, especially for the T-channel, for instance $L - M$ (Tansley and Boynton 1978), $0.96L - 1.28M$ (Guth *et al* 1980) or $0.8L - M$ (Stromeyer *et al* 1983). Naturally, the underlying problem is the disagreement about the relative contributions of L and M-cones to the T-channel (Mullen and Kingdom 1991).

3.2. Opponent modulation space

Let us again consider a background stimulus defined by its (L_0, M_0, S_0) components in the cone excitation space. We aim to compute the amplitudes $(\Delta A, \Delta T, \Delta D)$ associated with an incremental stimulus $(\Delta L, \Delta M, \Delta S)$ on the background. The general solution to the problem can be written in a compact form as follows (Brainard 1996):

$$\begin{pmatrix} \Delta A \\ \Delta T \\ \Delta D \end{pmatrix} = \begin{pmatrix} k_A & 0 & 0 \\ 0 & k_T & 0 \\ 0 & 0 & k_D \end{pmatrix} \times \begin{pmatrix} W_{A,L} & W_{A,M} & W_{A,S} \\ W_{T,L} & W_{T,M} & W_{T,S} \\ W_{D,L} & W_{D,M} & W_{D,S} \end{pmatrix} \begin{pmatrix} \Delta L \\ \Delta M \\ \Delta S \end{pmatrix}. \tag{26}$$

The $(\Delta A, \Delta T, \Delta D)$ amplitude space or *opponent modulation space* is also known in the literature as *DKL-space*, after Derrington, Krauskopf and Lennie (Derrington *et al* 1984). To compute the coefficients of the matrices in equation (26), the *ATD* channels are defined by the properties they must verify. For the A channel we will assume:

$$W_{A,L} = W_{A,M} = 1 \qquad W_{A,S} = 0. \tag{27}$$

The response of the T channel should not change before luminance-only changes, and consequently, before incremental stimuli proportional to the background. Furthermore, it is assumed that the S-cones do not contribute to this channel. Therefore

$$\Delta T = 0 \qquad \text{iff} \quad (\Delta L \;\; \Delta M \;\; \Delta S) = k(L_0 \;\; M_0 \;\; S_0) \tag{28}$$

$W_{T,S} = 0$.

From (26) and (28),

$$W_{T,M} = -W_{T,L}\frac{L_0}{M_0}. \tag{29}$$

Finally, the response of the D channel is assumed to be invariant before luminance-only changes and also before stimulus changes that do not alter either the response of the S-cones or the response of the achromatic channel:

$$\Delta D = 0 \qquad \text{if} \quad (\Delta L \;\; \Delta M \;\; \Delta S) = k(L_0 \;\; M_0 \;\; S_0)$$
$$\text{if} \quad \Delta A = 0 \quad \text{and} \quad \Delta S = 0 \quad \Rightarrow \quad \Delta D = 0. \tag{30}$$

With this condition on equation (25), it follows that

$$W_{D,M} = -\frac{W_{A,M}}{W_{A,L}} W_{D,L}$$
$$W_{D,S} = -\frac{L_0 + (W_{A,M}/W_{A,L})M_0}{S_0} W_{D,L}. \tag{31}$$

From all this, equation (25) finally takes the form

$$\begin{pmatrix} \Delta A \\ \Delta T \\ \Delta D \end{pmatrix} = \begin{pmatrix} k_A & 0 & 0 \\ 0 & k_T & 0 \\ 0 & 0 & k_D \end{pmatrix} \times \begin{pmatrix} 1 & 1 & 0 \\ 1 & -L_0/M_0 & 0 \\ -1 & -1 & (L_0 + M_0)/S_0 \end{pmatrix}^{-1} \begin{pmatrix} \Delta L \\ \Delta M \\ \Delta S \end{pmatrix} \tag{32}$$

where $k_A \equiv W_{A,M}$, $k_T \equiv W_{T,M}$ and $k_D \equiv W_{D,L}$. Note that the D channel, as defined by equation (32), differs in a global minus sign from that of Boynton's model (equation (24)). The choice of the sign reflects that the majority of the opponent blue–yellow cells are blue-on (Zrenner and Gouras 1981).

Different criteria, all equally arbitrary and therefore disputable, have been proposed to scale ΔA, ΔT and ΔD. Nevertheless, since the pooled contrast (Chaparro *et al* 1993), defined as

$$C = \sqrt{C_L^2 + C_M^2 + C_S^2} \tag{33}$$

where

$$C_L = \frac{\Delta L}{L_0} \qquad C_M = \frac{\Delta M}{M_0} \qquad C_S = \frac{\Delta S}{S_0} \tag{34}$$

is intimately linked with the chromatic detection thresholds (Poirson *et al* 1990), the following criterion is generally used: a unity contrast signal isolating a particular channel gives unity response in that channel. With this condition, the scaling constants become

$$k_A = \frac{\sqrt{3}}{L_0 + M_0}$$
$$k_T = \frac{\sqrt{L_0^2 + M_0^2}}{L_0(L_0 + M_0)} \tag{35}$$
$$k_D = \frac{1}{L_0 + M_0}$$

and finally (32) can be written as

$$\begin{pmatrix}\Delta A\\ \Delta T\\ \Delta D\end{pmatrix} = \frac{1}{L_0+M_0} \times \begin{pmatrix} \sqrt{3} & \sqrt{3} & 0 \\ \dfrac{\sqrt{L_0^2+M_0^2}}{L_0} & -\dfrac{\sqrt{L_0^2+M_0^2}}{M_0} & 0 \\ -1 & -1 & \dfrac{L_0+M_0}{S_0} \end{pmatrix} \times \begin{pmatrix}\Delta L\\ \Delta M\\ \Delta S\end{pmatrix}. \tag{36}$$

Note that (32) and (36) are background dependent. Thus, the $(\Delta A, \Delta T, \Delta D)$ amplitudes depend both on signal and background, or equivalently, on the quantities $(\Delta L/L_0, \Delta M/M_0, \Delta S/S_0)$ in the cone contrast space. Therefore, we can re-formulate (32) and (36) as follows:

$$\begin{pmatrix}\Delta A/k_A\\ \Delta T/k_T\\ \Delta D/k_D\end{pmatrix} = \begin{pmatrix} L_0 & M_0 & 0 \\ L_0 & -L_0 & 0 \\ -L_0 & -M_0 & L_0+M_0 \end{pmatrix} \begin{pmatrix}C_L\\ C_M\\ C_S\end{pmatrix} \tag{37}$$

$$\begin{pmatrix}\Delta A\\ \Delta T\\ \Delta D\end{pmatrix} = \frac{1}{L_0+M_0} \times \begin{pmatrix} L_0\sqrt{3} & M_0\sqrt{3} & 0 \\ \sqrt{L_0^2+M_0^2} & -\sqrt{L_0^2+M_0^2} & 0 \\ -L_0 & -M_0 & L_0+M_0 \end{pmatrix} \times \begin{pmatrix}C_L\\ C_M\\ C_S\end{pmatrix}. \tag{38}$$

To end the analysis of this representation space, we will pay special attention to equation (32). The matrix rows represent the components, in the cone excitation space, of the vectors defining the A, T and D mechanisms, called *mechanism vectors* (see table 2). On the other hand, if we solve equation (32) for the cone amplitudes

$$\begin{pmatrix}\Delta L\\ \Delta M\\ \Delta S\end{pmatrix} = \frac{1}{L_0+M_0} \begin{pmatrix} L_0 & M_0 & 0 \\ M_0 & -M_0 & 0 \\ S_0 & 0 & S_0 \end{pmatrix} \begin{pmatrix}\Delta A/k_A\\ \Delta T/k_T\\ \Delta D/k_D\end{pmatrix}. \tag{39}$$

The columns of the transformation matrix represent the components, in the cone excitation space, of the stimuli that isolate a mechanism, that is, those stimuli that yield zero response in two of the mechanisms and non-zero response in the remaining one. These stimuli (see again table 2) are called *stimulus vectors*. For simplicity, let us consider two mechanisms only: the achromatic or luminance mechanism, and the red–green chromatic mechanism. The achromatic mechanism vector is, by definition, orthogonal to the red–green stimulus vector, and analogously, the chromatic mechanism vector is orthogonal to the luminance stimulus vector. Nevertheless (see figure 8(*a*)), it is worth noting that the mechanism vectors are not mutually orthogonal, neither are the stimulus vectors. In other words, a purely achromatic stimulus, though giving zero response in the chromatic channels, does not give maximum response in the achromatic channel. The same would happen with a purely chromatic stimulus.

Analogously, the mechanism and stimulus vectors (see table 2 and figure 8(*b*)), may be defined from equation (37) and its corresponding inverse:

$$\begin{pmatrix}C_L\\ C_M\\ C_S\end{pmatrix} = \frac{1}{L_0+M_0} \begin{pmatrix} 1 & M_0/L_0 & 0 \\ 1 & -1 & 0 \\ 1 & 0 & 1 \end{pmatrix} \begin{pmatrix}\Delta A/k_A\\ \Delta T/k_T\\ \Delta D/k_D\end{pmatrix} \tag{40}$$

although we must bear in mind that the cone contrast space is not really a vector space, and so the terms mechanism and stimulus vectors are misnomers.

3.3. On the usefulness of differential transformations as colour representation spaces

Since the behaviour of the visual system is highly nonlinear, we will only be able to establish local (point-dependent) linear characterizations of colour perception. Despite this dependence on adaptation or surround, it should be possible to achieve a global characterization from a point-dependent one (the cone contrast space or the opponent modulation space, for instance) by integrating the local changes that take place when the stimuli are slightly modified.

For instance, let $\tilde{T}_0$ be a three-dimensional characterization of the response of the visual system, at a given physiological level, when it is adapted to a background stimulus characterized by the tristimulus vector T_0. Both the cone contrast and the opponent modulation representations ensure that the variation of the response, $\Delta\tilde{T}_0$, can be linearly related to the stimulus variation, ΔT_0, if $|\Delta T_0|$ is small. Therefore, in a neighbourhood of T_0 it holds that

$$\Delta\tilde{T}_0 = W(T_0)\,\Delta T_0 \tag{41}$$

or, in other words,

$$\mathrm{d}\tilde{T}_0 = W(T_0)\,\mathrm{d}T_0 \tag{42}$$

where $W(T_0)$ is a background-dependent matrix.

These relative or *differential characterizations* are empirical. They arise from the experimental studies on the visual system's response in conditions of adaptation at cone level or at LGN level, where the observers deal with incremental stimuli. However, from a theoretical perspective, it is desirable to have an absolute or *integrated characterization* of the response of the system to a given stimulus. This should be possible by integrating the incremental changes obtained when the stimulus is differentially modified.

A differential representation with a given background dependence in the local linear transformation, $W(T)$, will be an interesting colour representation space if equation (42) can be integrated, i.e. it *should be proved* that the elementary changes in the characterization of the response can be added straightforwardly. If it is so, we will have a well behaved representation: any change of the stimulus T_0 to give any arbitrary stimulus T_1, will modify the response of the system in this way,

$$\tilde{T}_1 = \tilde{T}_0 + \int_{\tilde{T}_0}^{\tilde{T}_1} \mathrm{d}\tilde{T} = \tilde{T}_0 + \int_{T_0}^{T_1} W(T)\,\mathrm{d}T. \tag{43}$$

Table 2.

	Mechanisms	Stimuli
Cone excitation space	A channel: $(1\ \ 1\ \ 0)$	Achromatic stimulus: $\frac{1}{L_0+M_0}\begin{pmatrix}L_0\\M_0\\S_0\end{pmatrix}$
	T channel: $(1\ \ -L_0/M_0\ \ 0)$	T stimulus $L-M$: $\frac{M_0}{L_0+M_0}\begin{pmatrix}1\\-1\\0\end{pmatrix}$
	D channel: $(-1\ \ -1\ \ (L_0+M_0)/S_0)$	D stimulus: $\frac{S_0}{L_0+M_0}\begin{pmatrix}0\\0\\1\end{pmatrix}$
Cone contrast space	A channel: $(L_0\ \ M_0\ \ 0)$	Achromatic stimulus: $\frac{1}{L_0+M_0}\begin{pmatrix}1\\1\\1\end{pmatrix}$
	T channel: $(L_0\ \ -L_0\ \ 0)$	T stimulus: $\frac{1}{L_0+M_0}\begin{pmatrix}M_0/L_0\\-1\\0\end{pmatrix}$
	D channel: $(-L_0\ \ -M_0\ \ L_0+M_0)$	D stimulus: $\frac{1}{L_0+M_0}\begin{pmatrix}0\\0\\1\end{pmatrix}$

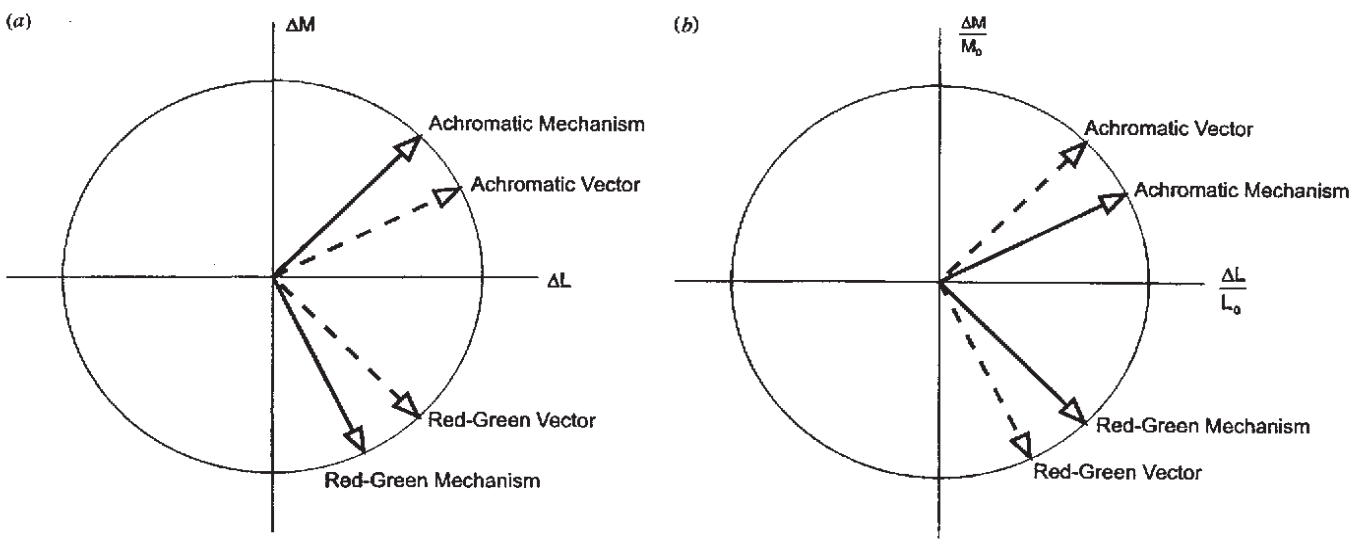

Figure 8. Mechanism and stimulus vectors defined from an achromatic background, represented in (*a*) the cone excitation space and (*b*) the cone contrast space.

Therefore, any arbitrary stimulus can be placed in the nonlinear representation, $\tilde{T}$, if the dependence of the transformation matrix on the background is known and some origin of the representation (a reference T_0 of known response $\tilde{T}_0$) is assumed.

Note that if the transformation is point independent, W could be out of the integral and equation (43) would reduce to a simple basis transformation and the $\tilde{T}$ characterization would be a tristimulus representation. Obviously, this is not the case, and the corresponding representation is no longer vectorial.

If equation (43), or any other more complex model of additivity, is not proposed and tested, the corresponding characterization of the incremental behaviour (equation (41)) will not be useful.

4. Third-stage spaces

The more recent colour models include a second transformation of the *ATD* signals, which would occur at the striate cortex, but it is not yet completely clear which cells support this transformation (Hubel and Wiesel 1968, Michael 1978a, b, Thorell *et al* 1984, Vautin and Dow 1985, Ts'o and Gilbert 1988, Lennie *et al* 1990). Examples of these models are those proposed by Guth (1991, 1993, 1994, 1995, 1998) and DeValois and DeValois (1993). Nevertheless, the treatment of the problem using Guth's model is complex, since it is not just a colour vision model, but also an adaptation model, including noise and gain control at the cone level, as well as nonlinearities in the

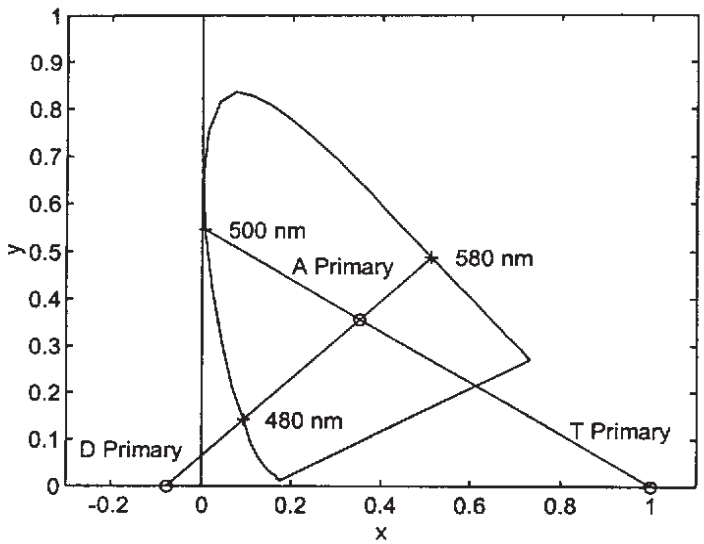

Figure 9. An *ATD* space (Ingling *et al* 1996) defined from the perceptual neutral axes. The intersection points of the zero luminous flux line and the perceptual neutral axes define the T and D primaries. The A primary is defined by the intersection point of the two neutral axes.

two opponent stages, both in the second and third stage. The transformations occurring at each stage cannot then be envisaged as a simple basis transformation. DeValois and DeValois's model, which does not fit into the typical *ATD* model scheme, is still, nevertheless, linear, with a second *cone opponent stage* and a third *perceptual opponent stage*. In the cone opponent stage, three opponent channels are generated (instead of one non-opponent and two opponent channels as in *ATD* models), approximately corresponding with the classical $L - M$, $M - L$ and $S - (L + M)$ channels, supported by the corresponding LGN cells. Linear combinations of these channels yield, in the third perceptual opponent stage, three perceptual channels, an achromatic and two chromatic channels. The main motive underlying the need for a third stage is the non-coincidence of the perceptual null axes with the cardinal directions (Krauskopf *et al* 1982) defined by the null axes of the LGN opponent cells.

Following a more traditional schema, Ingling *et al* (1996) have recently defined an *ATD*-space obtained as linear transformations of LMS, in such a way that the null axes of the T and D channels are, directly, the perceptual neutral axes, assuming that they are determined by wavelengths 480 and 580 nm for T, and by 500 and the point of (x, y) coordinates $(1, 0)$ for D. This implies a change of the D primary from the corresponding primary in Boynton's space (Boynton 1986). To compute the new primary (figure 9), it suffices to obtain the point verifying $A = T = 0$, that is, the intersecting point of the line connecting 480 nm to 580 nm and the zero luminous flux line ($y = 0$). The intersection occurs at $x = -0.0777$. The A primary also changes slightly, since the intersection of the two null axes, $T = D = 0$, is not exactly the equal-energy white. With all this, the matrix for the basis transformation from XYZ to this perceptual *ATD*-space is

$$\begin{pmatrix} A \\ T \\ D \end{pmatrix}_{\text{perc}} = \begin{pmatrix} k_1 & 0 & 0 \\ 0 & k_2 & 0 \\ 0 & 0 & k_3 \end{pmatrix} \times \begin{pmatrix} 0.3535 & 1 & -0.0777 \\ 0.3555 & 0 & 0 \\ 0.2920 & 0 & 1.0777 \end{pmatrix}^{-1} \begin{pmatrix} X' \\ Y' \\ Z' \end{pmatrix}. \tag{44}$$

In terms of the Smith and Pokorny fundamentals normalized to 100 at their peaks (see equation (22)), the equation defining the perceptual *ATD* channels as proposed by Ingling *et al* is

$$\begin{pmatrix} A \\ T \\ D \end{pmatrix}_{\text{perc}} = \begin{pmatrix} 0.637 & 0.392 & 0 \\ 3.44908 & -5.11065 & 1.31691 \\ 0.58782 & 0.36182 & -1.82701 \end{pmatrix}^{-1} \times \begin{pmatrix} L \\ M \\ S \end{pmatrix}. \tag{45}$$

From (45) and (44), we obtain that $k_1 = 35.5423$, $k_2 = 286.2934$ and $k_3 = -121.7975$.

This transformation mapping LMS to perceptual *ATD*, may be considered as the result of a third stage acting on the second stage of a LGN-based *ATD* model, let us say that of Boynton (1986). The matrix that would perform that operation is easier to interpret if the A primary defined in the model of Ingling *et al* is changed. To this end, we will consider that the D neutral axis is defined by 498 nm, instead of 500 nm, and the point $(1, 0)$, following Boynton's model. Proceeding in this fashion, equation (44)

becomes

$$\begin{pmatrix} A \\ T \\ D \end{pmatrix}_{\text{perc}} = \begin{pmatrix} k_1 & 0 & 0 \\ 0 & k_2 & 0 \\ 0 & 0 & k_3 \end{pmatrix} \times \begin{pmatrix} \frac{1}{3} & 1 & -0.0777 \\ \frac{1}{3} & 0 & 0 \\ \frac{1}{3} & 0 & 1.0777 \end{pmatrix}^{-1} \begin{pmatrix} X' \\ Y' \\ Z' \end{pmatrix} \tag{46}$$

where k_1, k_2 and k_3 are, as usual, arbitrary scaling constants. So, finally, the transformation mapping Boynton's second stage on the perceptual space results:

$$\begin{pmatrix} A \\ T \\ D \end{pmatrix}_{\text{perc}} = \begin{pmatrix} k_1' & 0 & 0 \\ 0 & k_2' & 0 \\ 0 & 0 & k_3' \end{pmatrix} \times \begin{pmatrix} 1.0000 & 0 & 0 \\ 0.0083 & 2.1483 & -0.2839 \\ 0 & 0 & 1.0000 \end{pmatrix} \begin{pmatrix} A \\ T \\ D \end{pmatrix}_{\text{LGN}} \tag{47}$$

where $k_1' = 3k_1$, $k_2' = k_2$ and $k_3' = -0.9279k_3$. It can be seen that, except for scale changes, this transformation modifies only the T channel.

5. Final remarks

The appearance of non-related colours, i.e. colours viewed in isolation, is well described, in general, by the perceptual attributes—brightness, hue and saturation—which can be computed in any of the spaces described in this work, particularly in the more advanced third-stage spaces, which explicitly consider the effect of adaptation. Nevertheless, as we have mentioned in the introduction, the appearance of related colours, i.e. colours seen in a scene, depends on many factors, illuminant, background and surround, for instance. To quantify the perceptual descriptors—brightness, lightness, hue, saturation and chroma—of these stimuli, as well as to evaluate how any of these change with any of the factors listed above, more elaborate models are needed. The *colour appearance models* (Richter 1980, Hunt 1982, 1987, 1991, Hunt and Pointer 1985, Seim and Valberg 1986, Nayatani *et al* 1987, 1990, Fairchild 1991, 1996, Fairchild and Berns 1993, Luo *et al* 1996) perform these tasks. Nevertheless, they do not attempt to follow the physiological stages constituting the visual process. At present, there is no *physiological* model with all the capabilities of the colour appearance models. This is, doubtless, one of the major challenges for colour vision researchers.

References

Balasubramanian R, Allebach J P and Bouman C A 1994 Color-image quantization with use of a fast binary splitting technique *J. Opt. Soc. Am.* A **11** 2777–86

Blinn J F 1993 NTSC: nice technology super color *IEEE Comput. Graph. Appl.* **13** 17–23

Boynton R M 1986 A system of photometry and colorimetry based on cone excitations *Color Res. Appl.* **11** 244–52

Boynton R M and Kambe N 1980 Chromatic difference steps of moderate size measured along theoretically critical axes *Color Res. Appl.* **5** 13–23

Boynton R M, Schafer W and Neun M E 1964 Hue-wavelength relation measured by color-naming method for three retinal locations *Science* **146** 666–8

Brainard D H 1996 Cone contrast and opponent modulation color spaces *Human Color Vision* ed P K Kaiser and R M Boynton (Washington, DC: Optical Society of America) pp 563–79

Brown W R J and MacAdam D L 1949 Visual sensitivities to combined chromaticity and luminance differences *J. Opt. Soc. Am.* **39** 808

Bumbaca F and Smith K C 1987 Design and implementation of a colour vision model for computer vision applications *Comput. Vision Graphics Image Process.* **39** 226–45

Chaparro A, Stromeyer C F, Huang E P, Kronauer R F and Eskew R T 1993 Colour is what the eye sees best *Nature* **361** 348–50

Creutzfeldt O D, Lee B B and Elepfandt A 1979 A quantitative study of the chromatic organisation and receptive fields of cells in the lateral geniculate body of the rhesus monkey *Exp. Brain Res.* **35** 527–45

DeMarco P, Pokorny J and Smith V C 1992 Full-spectrum cone sensitivity functions for X-chromosome-linked anomalous trichromats *J. Opt. Soc. Am.* A **9** 1465–76

DeMonasterio F M and Gouras P 1975 Functional properties of ganglion cells of the rhesus monkey retina *J. Physiol.* **251** 167–95

Derrington A M, Krauskopf J and Lennie P 1984 Chromatic mechanisms in lateral geniculate nucleus of macaque *J. Physiol.* **357** 241–65

DeValois R L, Abramov I and Jacobs G H 1966 Analysis of response patterns of LGN cells *J. Opt. Soc. Am.* **56** 966–77

DeValois R L and DeValois K K 1993 A multi-stage color model *Vision Res.* **33** 1053–65

Drum B 1983 Short-wavelength cones contribute to achromatic sensitivity *Vision Res.* **23** 1433–9

Dubrovin B A, Fomenko A T and Novikov S P 1984 Modern geometry: methods and applications *Geometry in Regions of a Space: Basic Concepts* (New York: Springer) ch 1, pp 1–60

Ebrahimi T and Kunt M 1998 Visual data compression for multimedia applications *Proc. IEEE* **86** 1109–25

Edwards C H 1973 Advanced calculus of several variables *Euclidean Space and Linear Mappings* (New York: Academic) ch 1

Eisner A and MacLeod D I A 1980 Blue cones do not contribute to luminance *J. Opt. Soc. Am.* **70** 121–3

Estévez O 1979 On the fundamental data-base of normal and dichromatic color vision *PhD Thesis* Universidad de Amsterdam

Fairchild M 1991 Formulation and testing of an incomplete chromatic-adaptation model *Color Res. Appl.* **16** 243–50

——1996 Refinement of the RLAB color space *Color Res. Appl.* **21** 338–46

Fairchild M D and Berns R S 1993 Image color-appearance specification through extension of CIELAB *Color Res. Appl.* **18** 178–90

Faugeras O D 1979 Digital image processing within the framework of a human visual model *Proc. IEEE* **A55P_27** 380–93

Gouras P 1968 Identification of cone mechanisms in monkey ganglion cells *J. Physiol.* **199** 533–47

Guth S L 1991 Model for color vision and light adaptation *J. Opt. Soc. Am.* A **8** 976–93

——1992 *J. Opt. Soc. Am.* A **9** 344 (erratum)

——1993 Unified model for human color perception and visual adaptation II *Proc. SPIE* **1913** 440–8

——1994 *ATD* model for color vision II: applications *Proc. SPIE* **2170** 153–62

——1995 Further applications of the *ATD* model for color vision *Proc. SPIE* **2414** 12–26

——1998 The *ATD* model as a uniform chromaticity space *Proc. CIM'98 Colour Imaging in Multimedia* pp 19–26

Guth S L, Donley N J and Marrocco R T 1969 On luminance additivity and related topics *Vision Res.* **9** 537–75
Guth S L, Massof R W and Benzschawel T 1980 Vector model for normal and dichromatic vision *J. Opt. Soc. Am.* **70** 197–212
Hubel D H and Wiesel T N 1968 Receptive fields and functional architecture of monkey striate cortex *J. Physiol.* **195** 215–43
Hunt R W G 1982 A model of colour vision for predicting colour appearance *Color Res. Appl.* **7** 95–112
——1987 A model of colour vision for predicting colour appearance in various viewing conditions *Color Res. Appl.* **12** 297–314
——1991 Revised colour-appearance model for related and unrelated colours *Color Res. Appl.* **16** 146–65
Hunt R W G and Pointer M R 1985 A colour-appearance transform for the CIE-1931 standard colorimetric observer *Color Res. Appl.* **10** 165–79
Hurvich L M and Jameson D 1957 An opponent-process theory of color vision *Psych. Rev.* **64** 384–404
Ingling C R, Barley J P and Ghani N 1996 Chromatic content of spectral lights *Vision Res.* **36** 2537–51
Ingling C R and Tsou B H P 1977 Orthogonal combination of three visual channels *Vision Res.* **17** 1075–82
Ingling C R Jr 1977 The spectral sensitivity of the opponent-color channels *Vision Res.* **17** 1083–9
Ingling C R Jr, Russell P W, Rea M S and Tsou B H P 1978 Red–green opponent spectral sensitivity: disparity between cancellation and direct matching methods *Science* **201** 1221–3
Jameson D and Hurvich L M 1955a Some quantitative aspects of an opponent-colors theory. I. Chromatic responses and spectral saturation *J. Opt. Soc. Am.* **45** 546–52
——1955b Some quantitative aspects of an opponent-colors theory. II. Brightness, saturation and hue in normal and dichromatic vision *J. Opt. Soc. Am.* **45** 602–16
——1968 Opponent-response functions related to measured cone photopigments *J. Opt. Soc. Am.* **58** 429–30
Judd D B 1951 Report of US secretariat committee on colorimetry and artificial daylight *CIE Proc. (Stockholm, 1951)* vol I, part 7 (Paris: Bureau Central de la CIE) p 11
Kaiser P K and Boynton R M 1996 *Human Color Vision* (Washington, DC: Optical Society of America) ch 7, pp 249–311
Kranda K and King-Smith P E 1979 Detection of coloured stimuli by independent linear systems *Vision Res.* **19** 733–45
Krauskopf P, Williams D R and Heeley D W 1982 Cardinal directions of color space *Vision Res.* **22** 1123–31
Lee J H, Chang B H and Kim S D 1994 Comparison of colour transformations for image segmentation *Electron. Lett.* **30** 1660–1
Lee B B, Valberg A, Tigwell D A and Tyrti J 1987 An account of responses of spectrally opponent neurons in macaque lateral geniculate nucleus to successive contrast *Proc. R. Soc.* B **230** 293–314
Léger A, Omachi T and Wallace G K 1991 JPEG still picture compression algorithm *Opt. Engng* **30** 947–54
Lennie O, Krauskopf J and Sclar G 1990 Chromatic mechanisms in striate cortex of macaque *J. Neurosci.* **10** 309–56
Liu N Y, Yan H and Martin P 1996 Segmentation of map image using opponent-color dimensions *Color Res. Appl.* **21** 115–20
Luo M R, Lo M C and Kuo W G 1996 The LLAB (l:c) colour model *Color Res. Appl.* **21** 412–29
MacLeod D I A and Boynton R M 1979 Chromaticity diagram showing cone excitation by stimuli of equal luminance *J. Opt. Soc. Am.* **69** 1183–6
Michael C R 1978a Color vision mechanisms in monkey striate cortex: dual-opponent cells with concentric receptive fields *J. Neurophysiol.* **41** 572–88
——1978b Color vision mechanisms in monkey striate cortex: simple cells with dual opponent-color receptive fields *J. Neurosci.* **41** 1233–49
Millan M S, Corbalán M, Romero J and Yzuel M J 1995 Optical pattern recognition based on color vision models *Opt. Lett.* **20** 1722–4
Mollen J D and Polden P G 1977 An anomaly in the response of the eye to light of short wavelengths *Phil. Trans. Soc.* B **278** 207–40
Mullen K T and Kingdom F A A 1991 Colour contrast in form perception *Vision and Visual Disfunction, Vol 6, The Perception of Colour* ed J R Cronly-Dillon (New York: MacMillan) pp 198–217
Nayatani Y, Hashimoto K, Takahama K and Sobagaki H 1987 A non-linear color-appearance model using Estévez–Hunt–Pointer primaries *Color Res. Appl.* **12** 231–42
Nayatani Y, Takahama K, Sobagaki H and Hashimoto K 1990 Color-appearance model and chromatic-adaptation transform *Color Res. Appl.* **15** 210–21
Poirson A B, Wandell B A, Varner D C and Brainard D H 1990 Surface characterizations of color thresholds *J. Opt. Soc. Am.* A **7** 783–9
Richter K 1980 Cube-root spaces and chromatic adaptation *Color Res. Appl.* **5** 25–43
Seim T and Valberg A 1986 Towards a uniform color space: a better formula to describe the Munsell and OSA color scales *Color Res. Appl.* **11** 11–24
Sharma G and Trusell H J 1997 Digital color imaging *IEEE Trans. Image Process.* **IP-6** 901–32
Smith V C and Pokorny J 1975 Spectral sensitivity of the foveal cone photopigments between 400 and 500 nm *Vision Res.* **15** 161–71
——1996 The design and use of a cone chromaticity space: a tutorial *Color Res. Appl.* **21** 375–83
Stochham T G 1972 Image processing in the context of a visual model *Proc. IEEE* **60** 828–42
Stockman A, MacLeod D I A and Johnson N E 1993 Spectral sensitivities of the human cones *J. Opt. Soc. Am.* A **10** 2491–521
Stromeyer C F, Cole G R and Kronauer R E 1985 Second-site adaptation in the red–green chromatic pathways *Vision Res.* **25** 219–37
Stromeyer C F, Kronauer E and Cole G R 1983 Adaptative mechanism controlling sensitivity to red–green chromatic flashes *Colour Vision: Physiology and Psychophysics* ed J D Mollon and L T Sharpe (London: Academic) pp 313–30
Tansley W and Boynton R M 1976 A line, not a space, represents visual distinctness of borders formed by different colors *Science* **191** 954–7
——1978 Chromatic border perception: the role of red- and green-sensitive cones *Vision Res.* **18** 683–97
Thorell L G, De Valois R L and Albrecht D G 1984 Spatial mapping of monkey V1 cells with pure color and luminance stimuli *Vision Res.* **24** 754–69
Ts'o D Y and Gilbert C D 1988 The organization of chromatic and spatial interactions in the primate striate cortex *J. Neurosci.* **8** 1712–28
Vautin R G and Dow B M 1985 Color cell groups in foveal striate cortex of the behaving macaque *J. Neurophysiol.* **54** 273–92
Vos J J 1978 Colorimetric and photometric properties of a 2° fundamental observer *Color Res. Appl.* **3** 125–8
Vos J J and Walraven P L 1971 On the derivation of the foveal receptor primaries *Vision Res.* **11** 799–818
Walraven P L 1961 On the Bezold–Brücke phenomenon *J. Opt. Soc. Am.* **51** 1113–6
——1974 A closer look at the tritanopic convergence point *Vision Res.* **14** 1339–43
Wan S J, Prusinkiewicz P and Wong S K M 1990 Variance-based color image. Quantization for frame buffer display *Color Res. Appl.* **15** 52–8
Wiesel T N and Hubel D H 1966 Spatial and chromatic interactions in the lateral geniculate body of the rhesus monkey *J. Neurophysiol.* **29** 1115–56

Wisowaty J J 1983 An action spectrum for the production of transient tritanopia *Vision Res.* **23** 769–74
Wooten B R and Werner J S 1978 Short-wave cone input to the red–green opponent channel *Vision Res.* **19** 1053–4
Wyszecki G and Stiles W S 1982 *Color Science* (New York: Wiley)
Zeki S M 1980 The representation of colours in the cerebral cortex *Nature* **284** 412–8
Zrenner E and Gouras P 1981 Characteristics of the blue sensitive cone mechanism in primate retinal ganglion cells *Vision Res.* **21** 1605–9